Original Article

Ketogenic Diet Enhances Delayed Wound Healing in Immunocompromised Rats: A Histological and Immunohistochemical Study

Noha R. M. Elswaidy[1], Rasha A. Abd Ellatif[2] and Marwa A. A. Ibrahim[1]

[1]Department of Histology and Cell Biology, [2]Department of Anatomy, Faculty of Medicine, Tanta University, Egypt

ABSTRACT

Introduction: Wound healing is a complicated process that can be affected by various factors. Glucocorticoids delay the process of wound healing by several mechanisms. The ketogenic diet could aid in the treatment of several skin diseases especially those associated with oxidative stress.

Aim of the Work: To examine the role of the ketogenic diet in enhancing the delayed wound healing of thin skin in glucocorticoid-immunocompromised rats.

Material and Methods: Twenty-four adult male albino rats were equally allocated into four groups: Control, excisional wound in normal rats, excisional wound in immunocompromised rats (0.1 mg/kg/day of dexamethasone subcutaneously for 30 days), and excisional wound in immunocompromised rats on ketogenic diet (75 % fat, 20 % protein, and 5 % carbohydrate). Wound samples were obtained on either the 7th or the 14th day and processed for different biochemical, histological, and immunohistochemical techniques.

Results: On both the 7th and 14th day, the wound of immunocompromised rats expressed a significant increase in both tissue malondialdehyde and myeloperoxidase compared with normal rats. The mean wound area was significantly larger, while both mean wound healing rate and mean epidermal thickness were significantly dropped compared with normal rats. A significant increase in collagen fiber deposition was associated with a significant reduction of the number of Ki67 positive cells and mean number of VEGF-positive blood vessels. The wound of immunocompromised rats on a ketogenic diet exhibited a significant restoration of most of the studied parameters, particularly on the 14th day.

Conclusions: The ketogenic diet enhanced delayed wound healing via suppressing oxidative stress, modulating inflammation and collagen deposition, promoting proliferation, and enhancing angiogenesis particularly on the 14th day.

Received: 13 June 2021, **Accepted:** 02 August 2021

Key Words: Delayed wound healing; ketogenic diet; Ki67; VEGF.

Corresponding Author: Marwa A. A. Ibrahim, MD Department of Histology and Cell Biology, Faculty of Medicine, Tanta University, Egypt, **Tel.**: +20 10 9918 6399, **E-mail:** marwa.ibrahim@med.tanta.edu.eg; maleox68@yahoo.com

ISSN: 1110-0559, Vol. 45, No. 4

INTRODUCTION

Wound healing is a complicated process that includes a series of independent and intersecting phases which starts with the hemostasis phase to stop blood loss followed by the inflammatory phase, in which cellular debris and combat infection are eliminated by the infiltrated immune cells. The proliferative phase then follows for restoration of the skin's barrier function through migration of keratinocytes and fibroblasts from the edges to the inside of the wound followed by their multiplication. Finally, the remodeling phase occurs when the dermis is reorganized, and the extracellular matrix is reformed to strengthen the wound area by minimizing scar tissue.[1,2]

Wound healing can be affected by various factors including host factors, wound properties, and other external influences. Some chronic wounds have often failed to move through the typical stages of healing which resulted in their entrance into a state of pathologic inflammation due to delayed, partial, or disorganized healing process.[3,4] Some drugs such as corticosteroids can slow down the healing process. Glucocorticoids can affect the process of wound healing by several mechanisms. They prevent the earliest manifestations of the inflammatory process, inhibit repair and proliferation of tissue, and act via their immunosuppressive activity by causing lymphocytopenia, neutrophilia, and counteracting the macrophages' activity[5,6] Therefore, glucocorticoids (particularly hydrocortisone) have been successfully employed in designing a model of delayed wound healing in immunocompromised rats.[5]

Dietary therapy has long been a promising treatment option for a range of clinical conditions, such as pain and inflammation. The ketogenic diet (KD) is a very high fat, very low carbohydrate diet in which fat accounts for 90% of calories and carbohydrate accounts for only 1% of calories. As a result, glucose availability is limited and metabolic adaption to fatty acid oxidation is forced.[7] KD's low carbohydrate content slows glucose metabolism and promotes ketolysis or the utilization of ketone bodies (acetone, acetoacetate, and b-hydroxybutyrate) as an alternative energy source.[8,9] Although the caloric and fat

 DOI: 10.21608/ejh.2021.80453.1504

intake is very high, KD consumption is associated with loss of weight in obese persons and improvement of their metabolic health.[10]

The identified cellular consequences and the currently proposed KD therapy mechanisms show that a mainly ketone-based metabolism can effectively lower inflammation and nociception in contrast to glucose-based metabolism.[11] Previous researches proved that KD plays an effective role in reducing inflammation in mouse models.[12,13] The evidence for the efficacy of KD in treating epilepsy, brain tumors, type 2 diabetes, and neurodegeneration is progressively growing over the past decade.[14,15] Physicians and scientists have shifted their focus in recent years to study the use of KD in the treatment of cardiovascular disease, autoimmune illness as well as sports and combat performance improvement.[16,17]

Besides, KD may aid in the treatment of several skin diseases especially those associated with oxidative stress such as acne, psoriasis, cutaneous malignancy, varicose ulcers, cutaneous allergic reactions, and drug-induced skin photosensitivity.[18] KD can help to increase the body's natural antioxidant defenses through various mechanisms, consequently, it can be used as a part of the protocol of treatment of the above-mentioned skin diseases.[19]

Taken together, this work is aimed to examine the role of the ketogenic diet in enhancing the delayed wound healing of thin skin in glucocorticoid-immunocompromised rats using different biochemical, histological, and immunohistochemical techniques.

MATERIAL AND METHODS

Experimental design

This study was permitted by the Research Ethics Committee of Tanta Faculty of Medicine, Egypt. Twenty-four adult male Wistar albino rats, weighing 150-170 grams each, were kept under standard housing conditions. The animals were equally allocated into four groups:

Group I (Control group): was equally subdivided into 2 subgroups; Animals of subgroup (Ia) were left untreated throughout the study period while being kept on a standard laboratory diet and animals of subgroup (Ib) were kept on a ketogenic diet throughout the study period.

Group II (Excisional wound in normal rats): Rats were anesthetized with a mixture of ketamine (20mg/kg) and xylazine (4mg/kg), got their back hair shaved and disinfected, then two punch wounds (6 mm wide, 2 mm deep) were induced in the interscapular area, each lateral to the midline. The rats were further subdivided into 2 subgroups; subgroup IIa, whose animals were euthanized with pentobarbital (40 mg/kg)[20] on the 7th day and subgroup IIb, whose animals were euthanized on the 14th day.

Group III (Excisional wound in immunocompromised rats): Rats were administered 0.1 mg/kg/day of dexamethasone subcutaneously for 30 days[5] while being kept on a standard laboratory diet. Afterwards, two punch wounds were induced as described in group II. The rats were further subdivided into 2 subgroups; subgroup IIIa, whose animals were euthanized on the 7th day and subgroup IIIb, whose animals were euthanized on the 14th day.

Group IV (Excisional wound in immunocompromised rats on a ketogenic diet): Rats were administered 0.1 mg/kg/day of dexamethasone subcutaneously for 30 days[5] while being concomitantly kept on a ketogenic diet (75 % fat, 20 % protein, and 5 % carbohydrate).[21] Afterwards, two punch wounds were induced as described in group II. Both dexamethasone intervention and ketogenic diet proceeded till the end of the study. The rats were further subdivided into 2 subgroups; subgroup IVa, whose animals were euthanized on the 7th day and subgroup IVb, whose animals were euthanized on the 14th day.

Biochemical study

Tissue malondialdehyde (MDA) level, a pro-oxidative marker, was measured through spectrophotometry.[22] Tissue myeloperoxidase (MPO) level, an index of the degree of polymorphic mononuclear cell accumulation, was assayed using a commercial ELISA kit.[23]

Histological preparation for light microscopy

Skin wound specimens were fixed with 10% neutral buffered formalin, washed, dehydrated, cleared, and paraffinized. Sections of 5µm thickness were stained with hematoxylin and eosin (H&E)[24] and Masson's trichrome stain.[25]

Immunohistochemical staining

Skin wound sections of 5 µm thickness were dewaxed, rehydrated, and washed. Thereafter, the sections were incubated overnight with the primary antibodies at 4°C; anti-Ki67 as a proliferation marker (ab15580; Abcam, Massachusetts, USA) and anti-vascular endothelial growth factor (VEGF) as an angiogenesis marker (RB-9031-P-A, Thermo Fisher Scientific, Massachusetts, USA). The sections were washed thrice and incubated with biotinylated goat anti-rabbit IgG for an hour. Streptavidin–biotin–horseradish peroxidase was added for another hour then washed thrice. Immunoreaction was visualized using 3,3'diaminobenzidine (DAB)-hydrogen peroxide. Counterstaining was done with Mayer's hematoxylin.[26]

Morphometric study

A Leica optical microscope attached to a Leica digital camera (Switzerland) was used for photomicrograph acquisition. Image analysis was done with "ImageJ" software (version 1.48v National Institute of Health, Bethesda, Maryland, USA). Five non-overlapping fields for every section at a magnification power of 400 were analyzed for:

1) Mean wound area, epidermal thickness, and the wound closure rate (%) which was calculated as (initial wound area–final wound area)/initial wound area) ×100.[27]

2) Mean area percentage of collagen fiber content.

3) Mean percentage of Ki67-immunohistochemical positive cells.

4) Mean number of vascular endothelial growth factor (VEGF)-positive blood vessels.

Statistical analysis

Data analysis was done with one-way analysis of variance (ANOVA) then Tukey's test using statistical package for social sciences statistical analysis software (IBM SPSS Statistics for Windows, IBM Corp, Version 22.0. Armonk, NY, USA). Differences were considered significant if the probability value (p) was less than 0.05.[28]

RESULTS

Biochemical findings

Tissue malondialdehyde (MDA) level in both subgroups IIIa and IIIb was significantly elevated ($p<0.001$) than both subgroups IIa and IIb respectively. Whereas both subgroups IVa and IVb were significantly reduced ($p<0.001$) than both subgroups IIIa and IIIb respectively, yet they were non-significantly different ($p=0.2545$, 0.9283 respectively) from both subgroups IIa and IIb respectively (Table 1).

Moreover, tissue myeloperoxidase (MPO) level in both subgroups IIIa and IIIb was significantly raised ($p<0.001$) than both subgroups IIa and IIb respectively. Whereas both subgroups IVa and IVb were significantly reduced ($p<0.001$) than both subgroups IIIa and IIIb respectively. Besides, subgroup IVa was still significantly higher ($p<0.001$) than subgroup IIa, while subgroup IVb was non-significantly different ($p=0.0963$) from subgroup IIb (Table 1).

Histological findings

H&E staining

Group I (Control group): Examination of H&E stained sections from both control subgroups revealed the normal histological structure of the epidermal and dermal layers of the thin skin separated by a well-defined folded dermo-epidermal junction. The epidermis was composed of stratified squamous epithelium formed mainly of keratinocytes arranged into four layers; The basal layer (stratum basale) was formed of low columnar cells with basal oval nuclei. The overlying layer (stratum spinosum) consisted of polyhedral cells with central rounded nuclei. The next layer (stratum granulosum) consisted of spindle-shaped cells with basophilic keratohyalin granules. Finally, the superficial non-cellular horny layer (stratum corneum) was formed of acidophilic scales. The dermis was composed of an outer papillary layer with abundant capillaries and connective tissue cells, whereas the inner reticular layer showed a denser connective tissue rich in fibers. The dermis had hair follicles and the associated sebaceous glands (Figure 1).

Group II (Excisional wound in normal rats): H&E stained sections from rats of subgroup IIa (7th day of the wound) showed that the wound area was covered by remnants of granulation tissue overlying thin epidermis with vacuolated keratinocytes and thin overlying keratin. The wound overlayed some spaces with inflammatory infiltrate of fibrin exudate and mononuclear cells. An ill-defined flattened dermo-epidermal junction was detected. The dermal appendages were absent underneath the wound area (Figure 2).

Subgroup IIb (14th day of the wound) revealed the wound area was covered with an apparently intact multilayered epidermis with few vacuolated keratinocytes covered with intact keratin. A well-defined partially folded dermo-epidermal junction was observed. Few mononuclear cells were encountered. The dermal appendages including hair follicles and sebaceous glands were frequently detected (Figure 3).

Group III (Excisional wound in immunocompromised rats): H&E stained sections from rats of subgroup IIIa (7th day of the wound) showed that the wound area was completely covered by granulation tissue overlaying an inflammatory infiltrate of mononuclear cells and blood vessels. The dermo-epidermal junction was absent. The dermal appendages were absent underneath the wound area (Figure 4).

Subgroup IIIb (14th day of the wound) revealed that the wound area was covered by remnants of granulation tissue overlying thin epidermis with vacuolated keratinocytes and thin overlying keratin. The wound overlayed spaces with an inflammatory infiltrate of fibrin exudate and mononuclear cells. An ill-defined flattened dermo-epidermal junction was detected. The dermal appendages were absent underneath the wound area (Figure 5).

Group IV (Excisional wound in immunocompromised rats on a ketogenic diet): H&E stained sections from rats of subgroup IVa (7th day of the wound) showed that the wound area was covered by remnants of granulation tissue being replaced by thin epidermis with vacuolated keratinocytes and very thin overlying keratin. The wound overlayed an inflammatory infiltrate of mononuclear cells and blood vessels. A well-defined flattened dermo-epidermal junction was detected. The dermal appendages were absent underneath the wound area (Figure 6).

Subgroup IVb (14th day of the wound) revealed that the wound area was covered with an apparently intact thin epidermis with a few vacuolated keratinocytes and intact keratin. A well-defined partially folded dermo-epidermal junction was observed. Some mononuclear cells were detected. The dermal appendages including hair follicles and sebaceous glands were frequently detected (Figure 7).

The mean wound area in both subgroups IIIa and IIIb was significantly larger ($p<0.001$) than both subgroups IIa and IIb respectively. Whereas both subgroups IVa and IVb were significantly reduced ($p<0.001$) than both subgroups IIIa and IIIb respectively, yet they did not significantly differ (p=0.0639, 0.1093 respectively) from

both subgroups IIa and IIb respectively. The calculated mean wound healing rate in both subgroups IIIa and IIIb was significantly dropped ($p<0.001$) than both subgroups IIa and IIb respectively, while both subgroups IVa and IVb were significantly accelerated ($p<0.001$) compared to both subgroups IIIa and IIIb respectively, which did not significantly vary (p=0.0825, 0.1639 respectively) from both subgroups IIa and IIb respectively (Table 1, Histogram 1 A,B).

Moreover, the mean epidermal thickness in both subgroups IIIa and IIIb was significantly diminished ($p<0.001$) than both subgroups IIa and IIb respectively. Whereas both subgroups IVa and IVb were significantly increased ($p<0.001$) compared to both subgroups IIIa and IIIb respectively. On the other hand, subgroup IVa was still significantly reduced ($p<0.001$) than subgroup IIa, yet subgroup IVb did not significantly differ ($p=0.3903$) from subgroup IIb (Table 1, Histogram 1 C).

Masson's trichrome staining

Masson's trichrome-stained sections from both control subgroups revealed few fine collagen fibers in both dermal papillary and reticular layers (Figure 8). Subgroups IIa and IIb showed an abundant amount of collagen fibers in the dermis (Figures 9,10 respectively). Whereas the dermis of subgroups IIIa and IIIb depicted an extensive amount of irregularly arranged collagen fibers in the dermis (Figures 11,12 respectively). On the other hand, the dermis of subgroups IVa and IVb revealed a moderate amount of collagen fibers (Figures 13,14 respectively).

The mean area percentage of collagen fiber content in both subgroups IIIa and IIIb was significantly elevated ($p<0.001$) than both subgroups IIa and IIb respectively. Whereas both subgroups IVa and IVb were significantly reduced ($p<0.001$) than both subgroups IIIa and IIIb respectively, yet both subgroups IVa and IVb were still significantly greater ($p<0.001$) than subgroups IIa and IIb respectively (Table 1, Histogram 1 D).

Ki67 immunohistochemical staining

Ki67 immunostained sections from both control subgroups showed many ki67-positive cells with a nuclear reaction in the basal cells layer (stratum basale) and the sebaceous glands (Figure 15). Subgroups IIa and IIb showed numerous ki67-positive cells in the basal cells layer and other epidermal layers in addition to the sebaceous glands (Figures 16,17 respectively). Whereas subgroups IIIa showed almost no ki67-positive cells in the epidermal layers and were mainly confined to the dermal inflammatory cells (Figure 18), while IIIb depicted only a few ki67-positive cells in the basal cells layer and other epidermal layers (Figure 19). On the other hand, subgroups IVa and IVb revealed many ki67-positive cells in the basal cells layer and other epidermal layers in addition to the sebaceous glands (Figures 20,21 respectively).

The mean percentage of Ki67-positive cells in both subgroups IIIa and IIIb was significantly reduced ($p<0.001$) than both subgroups IIa and IIb respectively. Whereas both subgroups IVa and IVb were significantly increased ($p<0.001$) than both subgroups IIIa and IIIb respectively. On the other hand, subgroup IVa was significantly dropped ($p<0.001$) with referral to subgroup IIa, yet subgroup IVb did not significantly differ ($p=0.1486$) from subgroup IIb (Table 1, Histogram 1 E).

VEGF immunohistochemical staining

VEGF immunostained sections from both control subgroups depicted many dermal VEGF-positive blood vessels in the form of a cytoplasmic reaction in their lining cells (Figure 22). Subgroups IIa and IIb showed numerous VEGF-positive blood vessels in the dermis (Figures 23,24 respectively). Whereas the dermis of subgroups IIIa and IIIb revealed some VEGF-positive blood vessels (Figures 25,26 respectively). On the other hand, the dermis of subgroups IVa and IVb depicted many VEGF-positive blood vessels (Figures 27,28 respectively).

The mean number of VEGF-positive blood vessels in both subgroups IIIa and IIIb was significantly diminished ($p<0.001$) than both subgroups IIa and IIb respectively. Whereas both subgroups IVa and IVb were significantly elevated ($p<0.001$) compared to both subgroups IIIa and IIIb respectively, yet they did not significantly vary ($p=0.0815$, 0.1072 respectively) from both subgroups IIa and IIb respectively (Table 1, Histogram 1 F).

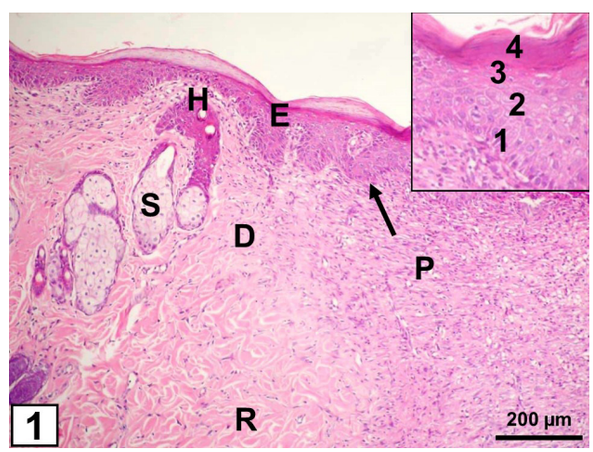

Fig. 1: Control subgroups show the normal histological structure of the epidermal (E) and dermal (D) layers of the thin skin separated by a well-defined folded dermo-epidermal junction (arrow). The epidermis is composed of stratified squamous epithelium formed mainly of keratinocytes arranged into four layers; stratum basale (1) is formed of low columnar cells with basal oval nuclei. Stratum spinosum (2) consists of polyhedral cells with central rounded nuclei. Stratum granulosum (3) consists of spindle-shaped cells with basophilic keratohyalin granules. Stratum corneum (4) is formed of acidophilic scales. The dermis is composed of an outer papillary (P) layer with abundant capillaries and connective tissue cells, the inner reticular (R) layer is composed of a denser connective tissue rich in fibers. The dermis contains hair follicles (H) and the associated sebaceous glands (S). (H&E x100, scale bar=200 µm, inset x 200)

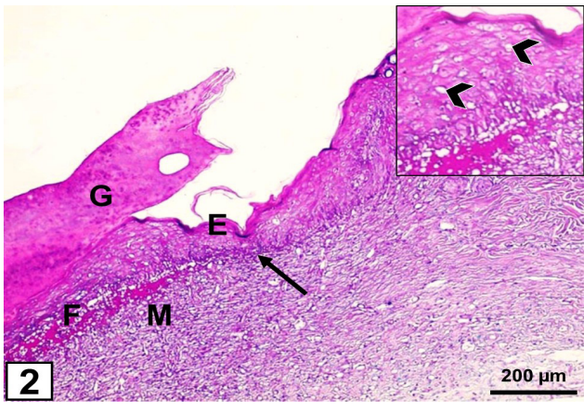

Fig. 2: Subgroup IIa (7th day of the wound) shows the wound area covered by remnants of granulation tissue (G) overlying thin epidermis (E) with vacuolated keratinocytes (arrowheads) and thin overlying keratin. The wound overlays spaces with an inflammatory infiltrate of fibrin exudate (F) and mononuclear cells (M). An ill-defined flattened dermo-epidermal junction (arrow) is detected. (H&E x100, scale bar=200 µm, inset x 200)

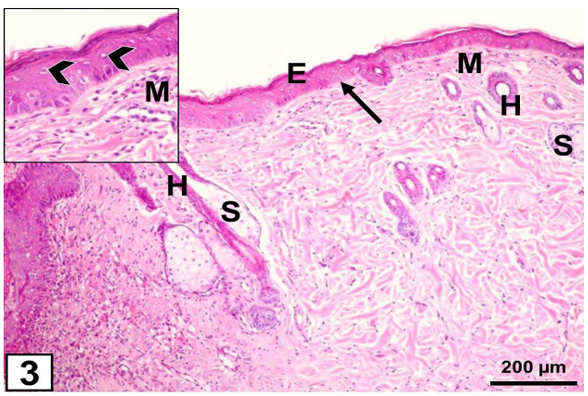

Fig. 3: Subgroup IIb (14th day of the wound) shows the wound area covered with an apparently intact multilayered epidermis (E) with few vacuolated keratinocytes (arrowheads) covered with intact keratin. A well-defined partially folded dermo-epidermal junction (arrow) is observed. Few mononuclear cells (M) are encountered. The dermal appendages including hair follicles (H) and sebaceous glands (S) are frequently detected. (H&E x100, scale bar=200 µm, inset x 200)

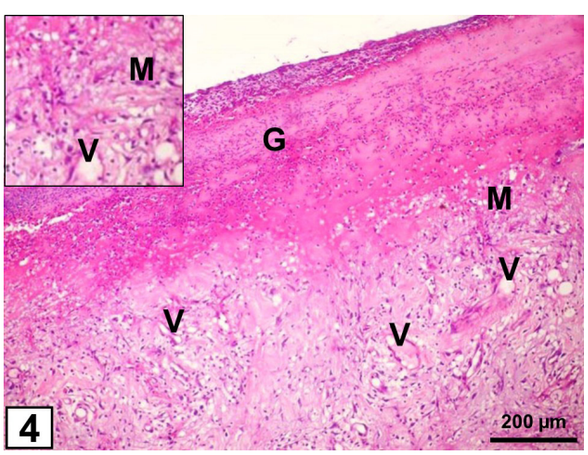

Fig. 4: Subgroup IIIa (7th day of the wound) shows the wound area completely covered by granulation tissue (G) overlaying an inflammatory infiltrate of mononuclear cells (M) and blood vessels (V). (H&E x100, scale bar=200 µm, inset x 200)

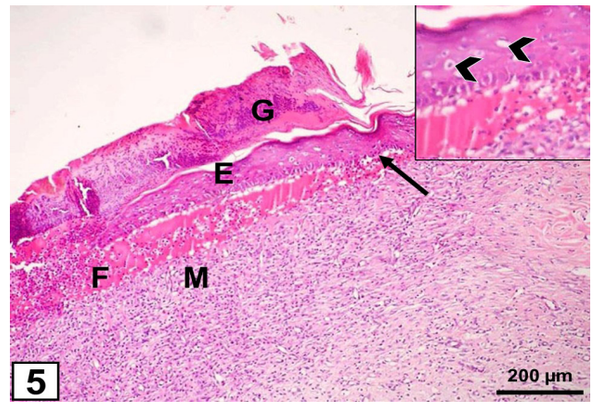

Fig. 5: Subgroup IIIb (14th day of the wound) shows the wound area covered by remnants of granulation tissue (G) overlying thin epidermis (E) with vacuolated keratinocytes (arrowheads) and thin overlying keratin. The wound overlays some spaces with an inflammatory infiltrate of fibrin exudate (F) and mononuclear cells (M). An ill-defined flattened dermo-epidermal junction (arrow) is detected. (H&E x100, scale bar=200 µm, inset x 200)

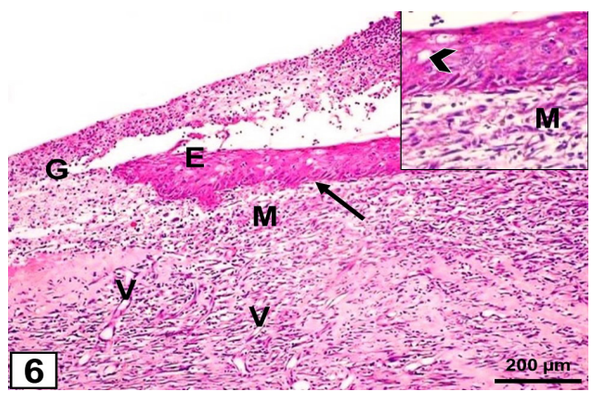

Fig. 6: Subgroup IVa (7th day of the wound) shows the wound area covered by remnants of granulation tissue (G) being replaced by thin epidermis (E) with vacuolated keratinocytes (arrowhead) and very thin overlying keratin. The wound overlays an inflammatory infiltrate of mononuclear cells (M) and blood vessels (V). A well-defined flattened dermo-epidermal junction (arrow) is detected. (H&E x100, scale bar=200 µm, inset x 200)

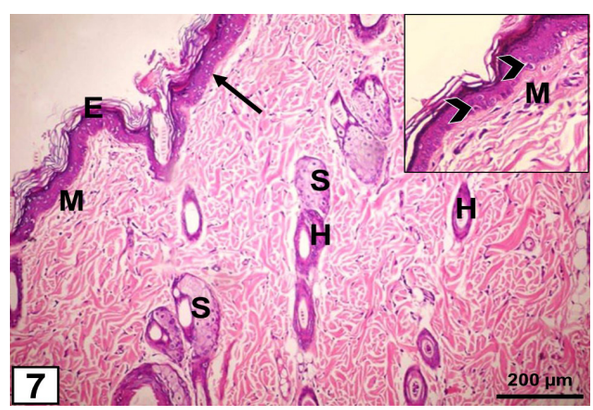

Fig. 7: Subgroup IVb (14th day of the wound) shows the wound area covered with an apparently intact thin epidermis (E) with a few vacuolated (arrowheads) and intact keratin. A well-defined partially folded dermo-epidermal junction (arrow) is observed. Some mononuclear cells (M) are detected. The dermal appendages including hair follicles (H) and sebaceous glands (S) are frequently detected. (H&E x100, scale bar=200 µm, inset x 200)

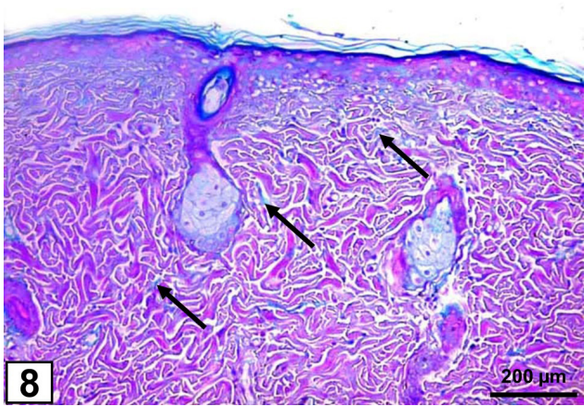

Fig. 8: Control subgroups show few fine collagen fibers (arrows) in both dermal papillary and reticular layers. (Masson's trichrome stain x100, scale bar=200 µm)

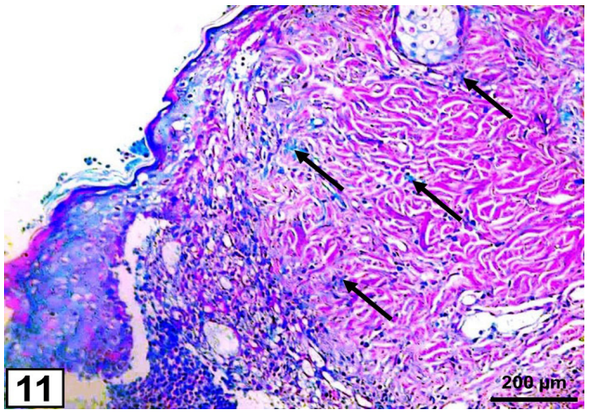

Fig. 11: Subgroup IIIa (7th day of the wound) shows an extensive amount of irregularly arranged collagen fibers (arrows) in the dermis. (Masson's trichrome stain x100, scale bar=200 µm)

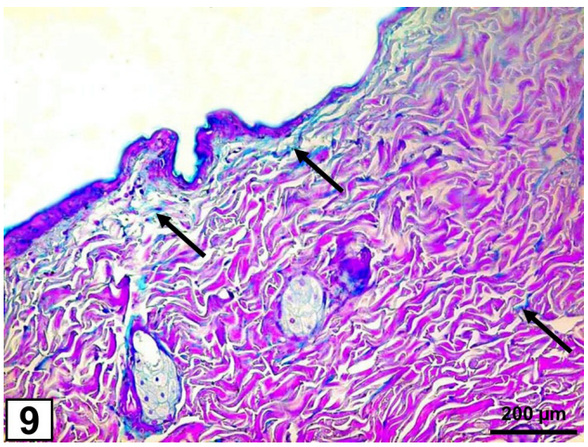

Fig. 9: Subgroup IIa (7th day of the wound) shows an abundant amount of collagen fibers (arrows) in the dermis. (Masson's trichrome stain x100, scale bar=200 µm)

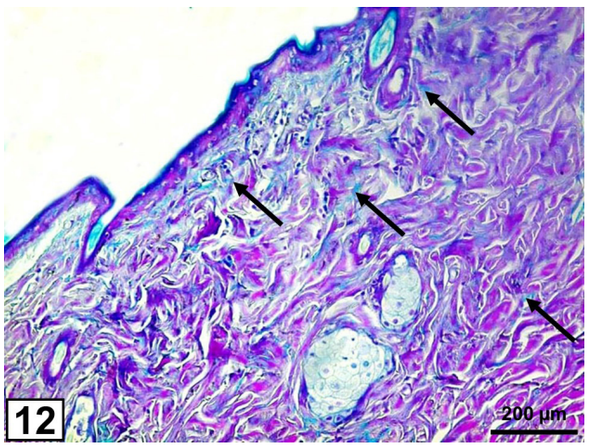

Fig. 12: Subgroup IIIb (14th day of the wound) shows an extensive amount of irregularly arranged collagen fibers (arrows) in the dermis. (Masson's trichrome stain x100, scale bar=200 µm)

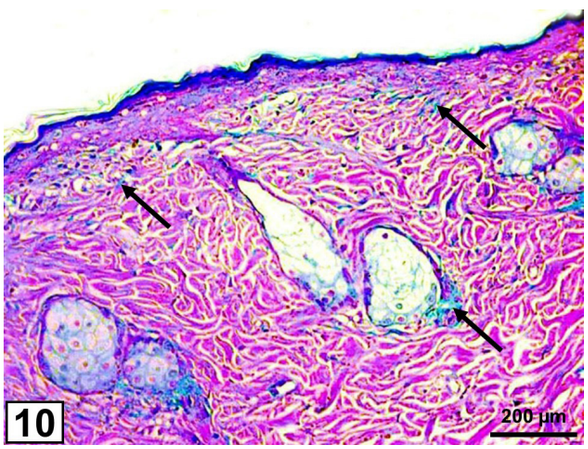

Fig. 10: Subgroup IIb (14th day of the wound) shows an abundant amount of collagen fibers (arrows) in the dermis. (Masson's trichrome stain x100, scale bar=200 µm)

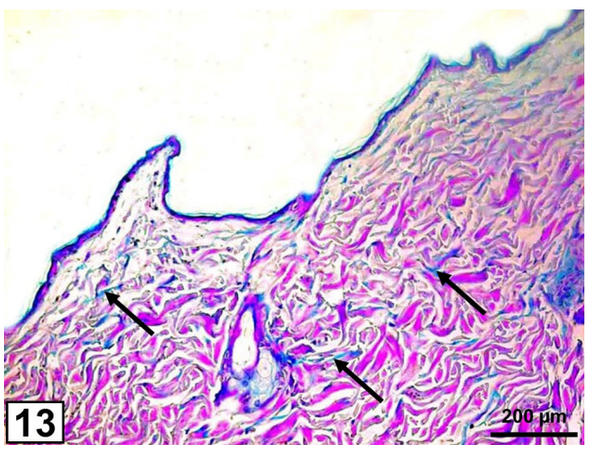

Fig. 13: Subgroup IVa (7th day of the wound) shows a moderate amount of collagen fibers (arrows) in the dermis. (Masson's trichrome stain x100, scale bar=200 µm)

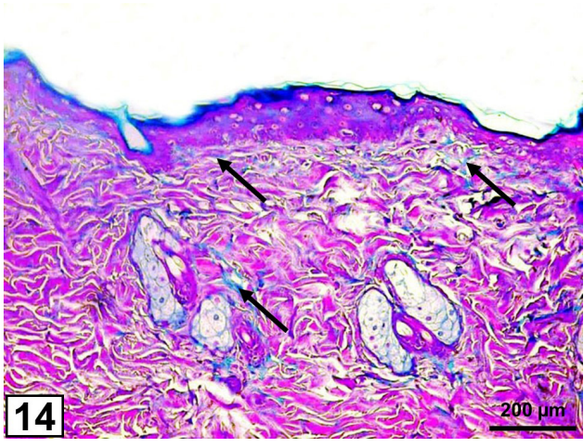

Fig. 14: Subgroup IVb (14th day of the wound) shows a moderate amount of collagen fibers (arrows) in the dermis. (Masson's trichrome stain x100, scale bar=200 µm)

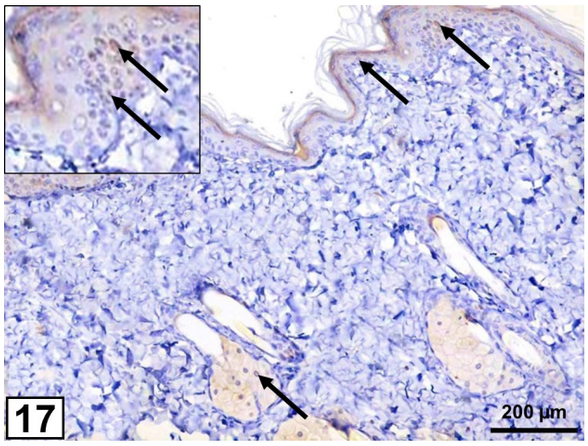

Fig. 17: Subgroup IIb (14th day of the wound) shows numerous ki67-positive cells (arrows) in the basal cells layer and other epidermal layers in addition to the sebaceous glands. (Ki67 x100, scale bar=200 µm, inset x 200)

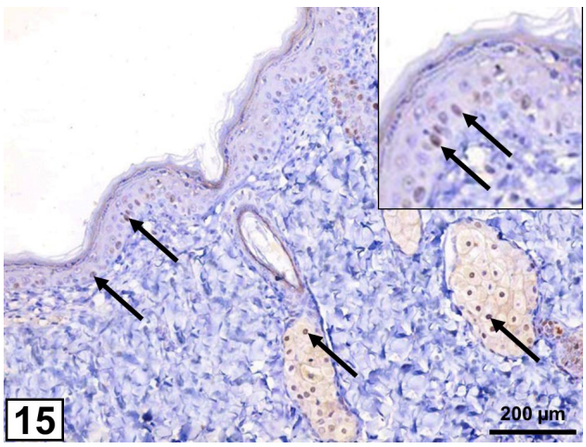

Fig. 15: Control subgroups show many ki67-positive cells (arrows) with a nuclear reaction in the stratum basale and the sebaceous glands. (Ki67 x100, scale bar=200 µm)

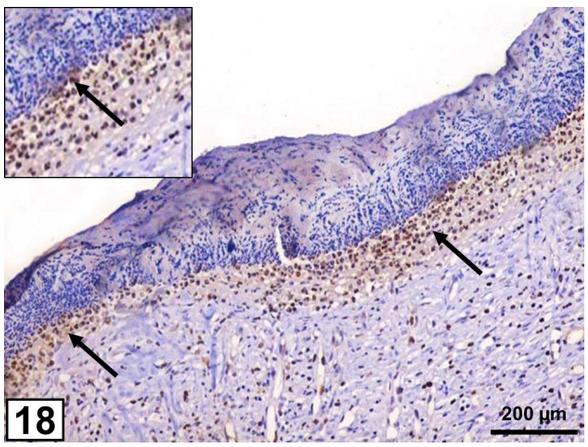

Fig. 18: Subgroup IIIa (7th day of the wound) shows almost no ki67-positive cells in the epidermal layers and mainly confined to the dermal inflammatory cells (arrows). (Ki67 x100, scale bar=200 µm, inset x 200)

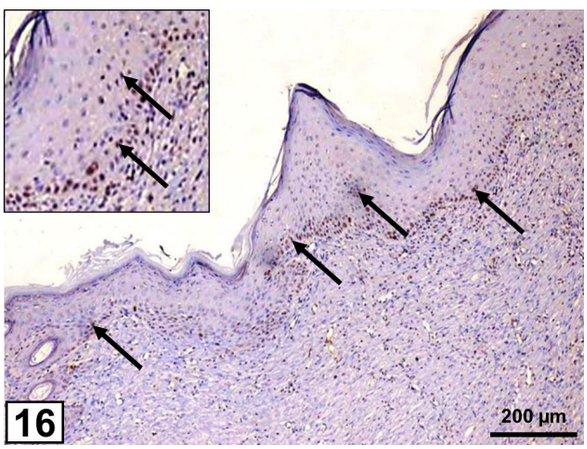

Fig. 16: Subgroup IIa (7th day of the wound) shows numerous ki67-positive cells (arrows) in the basal cells layer and other epidermal layers. (Ki67 x100, scale bar=200 µm, inset x 200)

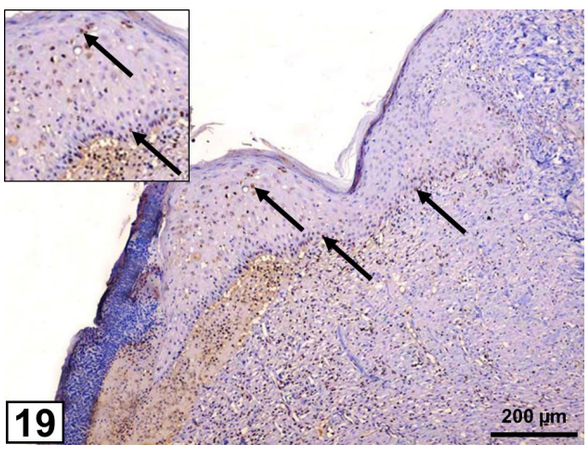

Fig. 19: Subgroup IIIb (14th day of the wound) shows few ki67-positive cells in the basal cells layer and other epidermal layers. (Ki67 x100, scale bar=200 µm, inset x 200)

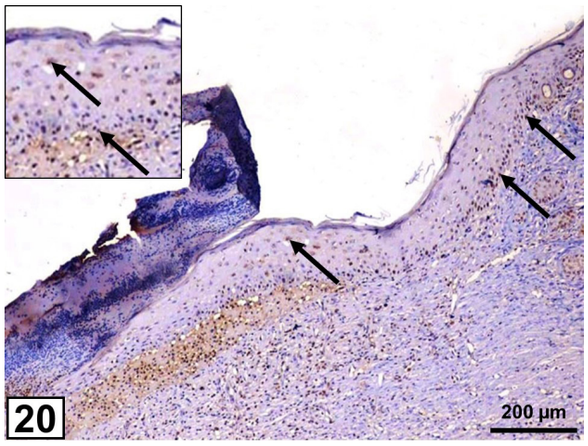

Fig. 20: Subgroup IVa (7th day of the wound) shows many ki67-positive cells (arrows) in the basal cells layer and other epidermal layers. (Ki67 x100, scale bar=200 µm, inset x 200)

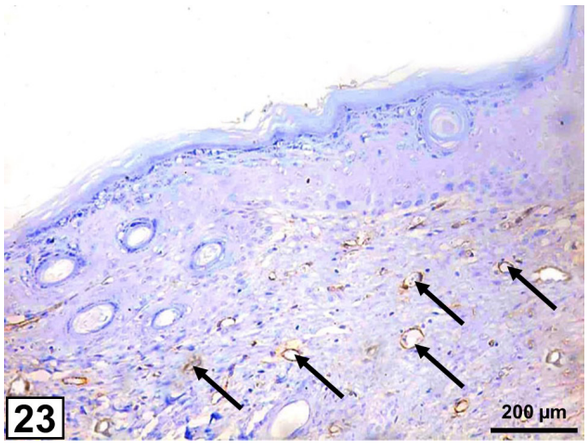

Fig. 23: Subgroup IIa (7th day of the wound) shows numerous VEGF-positive blood vessels (arrows) in the dermis. (VEGF x100, scale bar=200 µm)

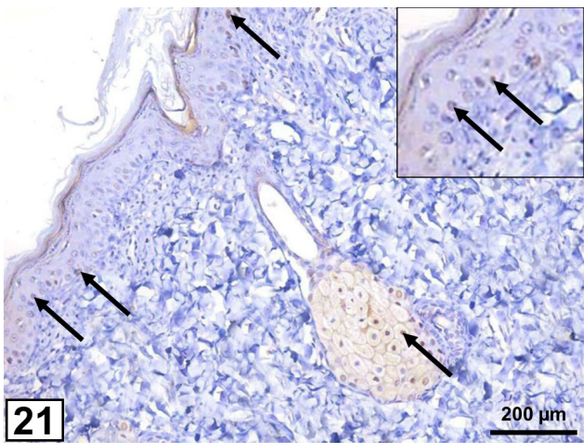

Fig. 21: Subgroup IVb (14th day of the wound) shows many ki67-positive cells (arrows) in the basal cells layer and other epidermal layers in addition to the sebaceous glands. (Ki67 x100, scale bar=200 µm, inset x 200)

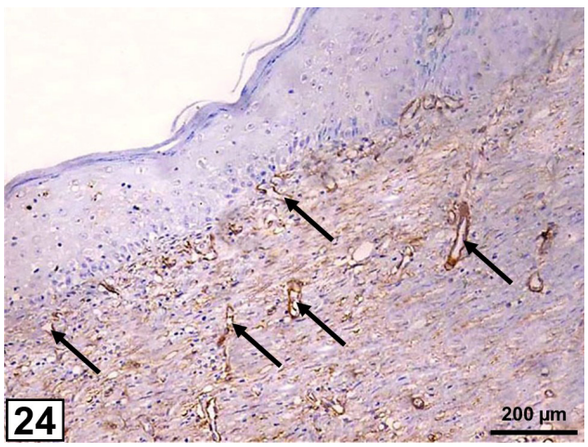

Fig. 24: Subgroup IIb (14th day of the wound) shows numerous VEGF-positive blood vessels (arrows) in the dermis. (VEGF x100, scale bar=200 µm)

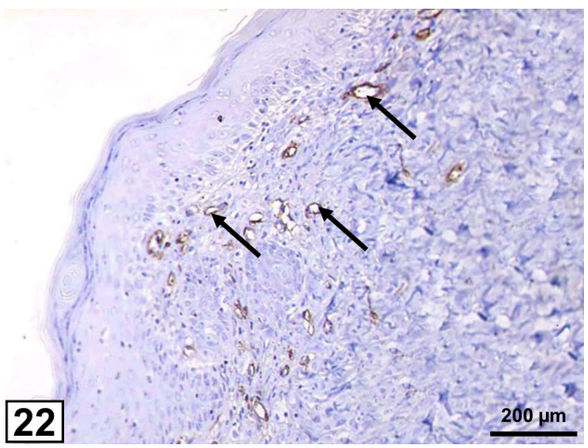

Fig. 22: Control subgroups show many dermal VEGF-positive blood vessels (arrows) in the form of a cytoplasmic reaction in their lining cells. (VEGF x100, scale bar=200 µm)

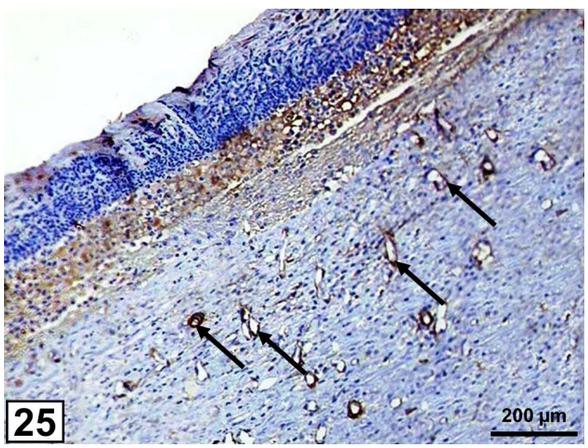

Fig. 25: Subgroup IIIa (7th day of the wound) shows some VEGF-positive blood vessels (arrows) in the dermis. (VEGF x100, scale bar=200 µm)

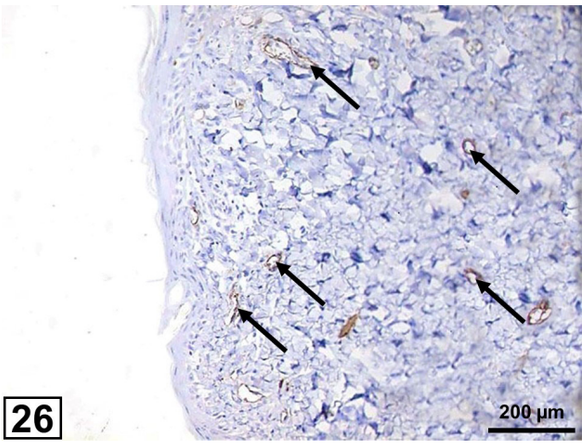

Fig. 26: Subgroup IIIb (14th day of the wound) shows some VEGF-positive blood vessels in the dermis. (VEGF x100, scale bar=200 µm)

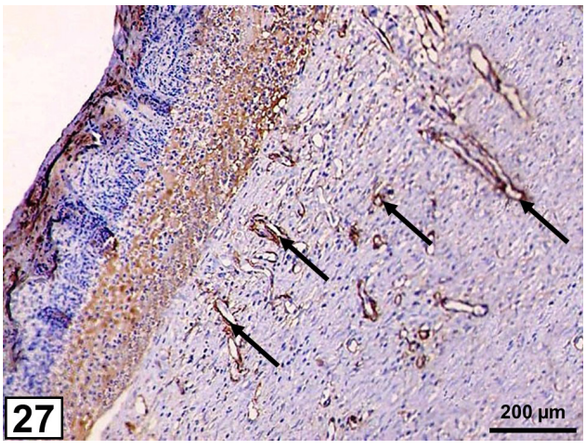

Fig. 27: Subgroup IVa (7th day of the wound) shows many VEGF-positive blood vessels (arrows) in the dermis. (VEGF x100, scale bar=200 µm)

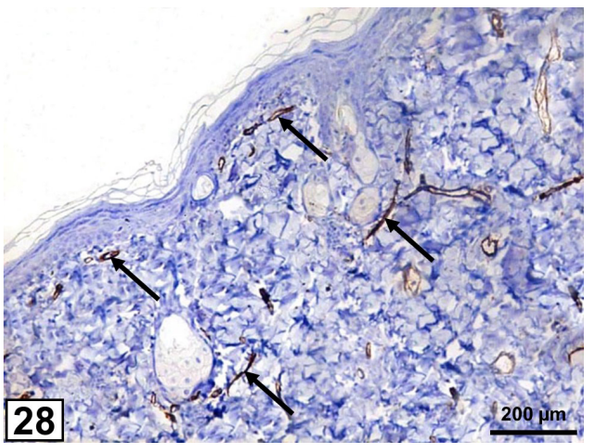

Fig. 28: Subgroup IVb (14th day of the wound) shows many VEGF-positive blood vessels (arrows) in the dermis. (VEGF x100, scale bar=200 µm)

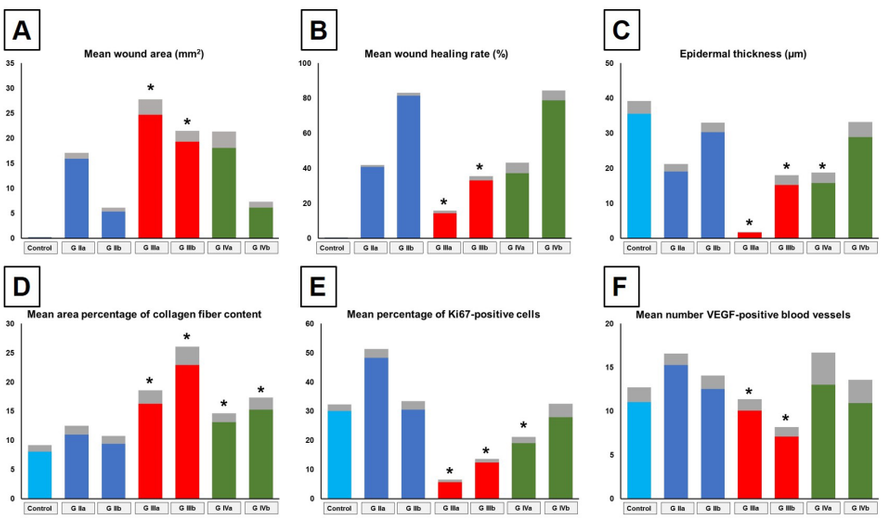

Histogram 1: Morphometrical and statistical analysis of [A] Mean wound area (mm2) [B] Mean wound healing rate (%) [C] Epidermal thickness (µm) [D] Mean area percentage of collagen fiber content [E] Mean percentage of Ki67-positive cells [F] Mean number VEGF-positive blood vessels. * denotes $p<0.05$ versus group II subgroups.

Table 1: Biochemical and morphometrical analysis

	Group I	Group II		Group III		Group IV	
		IIa	IIb	IIIa	IIIb	IVa	IVb
MDA nmol/g-tissue protein	58.37±3.24	65.67±5.66	60.88±4.28	88.64±6.58[a,c]	80.22±5.40[a,c]	69.26±7.81[b]	61.09±5.89[b]
MPO ng/mg tissue protein	4.49±0.15	8.57±1.12	5.26±0.94	17.19±1.97[a,c]	14.08±0.90[a,c]	12.09±2.66[a,b]	6.81±2.63[b]
Mean wound area (mm^2)	0	15.92±1.15	5.34±0.82	24.67±3.10[a,c]	19.30±2.15[a,c]	18.09±3.28[b]	6.11±1.19[b]
Mean wound healing rate (%)	0	40.76±1.15	81.47±1.65	14.40±1.41[a,c]	33.03±2.5[a,c]	37.23±5.96[b]	78.76±5.67[b]
Epidermal thickness (μm)	35.58±3.64	19.08±2.10	30.34±2.64	1.61±0.21[a,c]	15.22±2.81[a,c]	15.79±2.96[a,b]	28.94±4.28[b]
Mean area percentage of collagen fiber content	8.06±1.15	11.01±1.5	9.41±1.33	16.27±2.31[a,c]	22.88±3.17[a,c]	13.10±1.56[a,b]	15.24±2.09[a,b]
Mean percentage of Ki67-positive cells	30.09±2.21	48.22±3.1	30.52±2.91	5.64±0.9[a,c]	12.46±1.24[a,c]	19.06±2.07[a,b]	27.89±4.68[b]
Mean number VEGF-positive blood vessels	11.03±1.7	15.28±1.29	12.55±1.51	10.05±1.32[a,c]	7.09±1.08[a,c]	13.01±3.67[b]	10.91±2.66[b]

Data are expressed as mean ± standard deviation. a, b, c denote $p<0.05$ vs group II, III, and IV respectively of the corresponding subgroup.

DISCUSSION

In the present work, tissue MDA level in the excisional wound of immunocompromised rats was significantly higher than its level in the excisional wound in normal rats. This finding coincided with previous researches.[6] Recent studies attributed the elevated MDA level to the promoted peroxidation of cell membranes and subsequent alterations of their lipid structure. Corticosteroids can induce oxidative stress through the production of free radicals with subsequent oxidative DNA damage, peroxidation of membrane biomolecules, and cell death.[29] In addition, the balance between free radicals and antioxidants may be disrupted in wounding with reduction of the antioxidants[30]

On the other hand, MDA level in the excisional wound of immunocompromised rats on KD was significantly decreased compared with the wound of immunocompromised rats. The dropped level of MDA after use of KD was previously related to the induction of β-hydroxybutyric acid that inhibits class-I Histone, resulting in an increased acetylation at the Foxo3a and Mt2 promoters of genes that suppress oxidative stress.[31] Moreover, Ketone utilization can reduce the production of reactive oxygen species (ROS) by controlling the balance between oxidized and reduced forms of NAD to enhance mitochondrial function.[32]

In this study, MPO level in the wound of immunocompromised rats was significantly higher than in the wound of normal rats. The heme protein myeloperoxidase (MPO) is a major active component in activated neutrophils and monocytes.[33] The MPO enzyme assay is a reliable diagnostic tool for monitoring the progression of wound healing,[34] where the increase in the activity of MPO is the first response to inflammation starting instantly after the wounding process, as a defense mechanism of the tissue.[35] The inflammatory phase is the first and essential stage in the wound healing process. However, prolonged inflammation, as in immunocompromised state, enhances the release of cytokines such as IL-1β, IL-6, and TNF-α which results in serious healing disturbances, extensive fibrosis, and scarring,[36] particularly through the production and induction of proteolytic enzymes and arachidonic acid metabolites, thus delaying the initiation of the repair phase[37]

On the contrary, the wound of immunocompromised rats on KD revealed a significant decrease in tissue MPO compared to the wound of immunocompromised rats. Several studies explained this finding by the ability of the KD to reduce circulating some inflammatory markers including TNF-a, IL-6, IL-8, MCP-1, E-selectin, I-CAM, and PAI-1.[38,39] Pretreatment with KD was previously shown to significantly reduce subcutaneous inflammation in both juvenile and adult animals, where ketone metabolism can decrease the production of reactive oxygen species which contribute to inflammation.[8]

Moreover, in this work, immunocompromised rats showed a significant delay in the process of wound healing when examined at the 7th and the 14th day compared with normal rats as confirmed by measuring the mean wound area and calculating the mean wound healing rate, in addition to the mean epidermal thickness which was significantly lower than that in normal rats. Similar findings were previously reported.[40] These changes were previously attributed to the ability of corticosteroids to reduce inflammation, with subsequent affection of cell migration, proliferation, and angiogenesis resulting in delayed wound healing.[41]

On the other hand, immunocompromised rats on KD showed a significant improvement of the wound state particularly on the 14th day, where the wound area was covered with an apparently intact thin epidermis, intact keratin, well-defined dermo-epidermal junction, and the appearance of the dermal appendages. Besides, the mean wound area, wound healing rate, and epidermal thickness were significantly restored. Similarly, ketone supplementation in *vivo* and in *vitro* was proven to modify systemic physiology to enhance wound closure and was thus hypothesized that exogenous ketone supplementation could enhance metabolic and physiological features to boost healing in age-associated impaired wound healing.[42]

In the current work, the wound of immunocompromised rats revealed an extensive amount of irregularly arranged collagen fibers in the dermis. Researchers have reported that the formation of pathological scar is mainly due to excessive collagen deposition.[1] Fibroblasts (FBs) and myofibroblasts (MFs) play a crucial role during the healing process through secreting and remodeling of the extracellular matrix mainly collagen proteins.[43,44] In the early phases of wound healing, FBs proliferate and undergo phenotypic changes into MFs in response to mechanical tension and cytokines, especially transforming growth factor-β that are produced by inflammatory cells migrated to the wound area and result in increased collagen synthesis and contraction of wound edges.[2] In the remodeling phase, collagen is constantly degraded to decrease wound thickness and bring the wound margins closer together.[45] Moreover, the extensive amount of irregularly arranged collagen fibers may be correlated to the oxidative stress state and free radicals that play an important role in skin fibrosis.[46]

On the other hand, in the current work, collagen deposition in the wound of immunocompromised rats on KD was significantly lower than in the immunocompromised rats. This was previously related to the role of KD in regulating ROS levels, in addition to its anti-inflammatory effect, thus suppressing the excessive amount of collagen which is critical for optimal wound healing.[8,47]

In the current work, the wound of immunocompromised rats showed almost no ki67-positive cells in the epidermal layers and was mainly confined to the dermal inflammatory cells. Ki67 antigen is the most reliable marker of proliferating cells. The expression of proliferation marker, Ki67 should be increased in damaged skin.[48] Glucocorticoids were proven to have antiproliferative effects in many normal and tumor cell systems through a G1-block in the progression of the cell cycle,[49] thus explaining the low expression of Ki67 in the wound of immunocompromised rats.

On the other hand, the wound of immunocompromised rats on KD revealed a significant increase in ki67-positive cells compared with the immunocompromised rats, particularly on the 14th day. KD was suggested to elicit cellular proliferation similar to that of coconut oil which is a natural source of medium-chain triglycerides (MCTs) with a proven capacity to modulate cellular proliferation, cell signaling, and growth factor activities.[50]

Wound microenvironment mimics a hypoxic condition for injured cells that triggers expression of HIF-1α, resulting in promoting a transcriptional program that modulates cellular metabolism, redox homeostasis, vascular remodeling, and inflammation. HIF-1α binds to particular sequences of DNA that regulate VEGF expression, thus stimulating angiogenesis.[51,52] Angiogenesis is essential in the process of wound healing to support the new granulation tissue, the survival of keratinocytes, and re-epithelialization through the delivery of nutrients and oxygen to the wounded area.[53,54]

The present study demonstrated a significant drop in dermal VEGF immunoexpression in the wound of immunocompromised rats. This finding was in accordance with some investigators in response to the suppressive effect of corticosteroids.[4,55] On the other hand, the wound of immunocompromised rats on KD revealed numerous VEGF-positive blood vessels. It was previously established that new microvascular patterns with an increase in capillary density, similar to hypoxia-induced angiogenesis, occurred in the brain of rats fed on KD,[56] thus was explained as an angiogenic response to ketosis.

CONCLUSIONS

It could be concluded that KD enhances delayed wound healing via suppressing oxidative stress, modulating inflammation and collagen deposition, promoting proliferation, and enhancing angiogenesis particularly on the 14th day.

CONFLICT OF INTERESTS

There are no conflicts of interest.

REFERENCES

1. Zhao B, Zhang Y, Han S, Zhang W, Zhou Q, Guan H, Liu J, Shi J, Su L, Hu D. Exosomes derived from human amniotic epithelial cells accelerate wound healing and inhibit scar formation. J Mol Histol 2017;48:121–32.
2. Ismail D, Aboulkhair A. Histological Evaluation of the Emerging Role of Adipose Stem Cells-Derived Exosomes in Cutaneous Wound Healing in Albino Rats. Egypt J Histol 2018;41:459–72.
3. Guo S, Dipietro LA. Factors affecting wound healing. J Dent Res 2010;89:219–29.
4. Ibrahim NA. The possible protective effect of bee propolis on experimentally mediated cisplatin reproductive toxicity. Egypt J Histol 2013;36:78–86.
5. Monteiro BS, Faria RD, Zanella ARC, Cruz EP, Godoi NP, Fiorio WAB, Lenz D, Fortunato VR. Mesenchymal stem cell infusion on skin wound healing of dexamethasone immunosuppressed wistar rats. Ciência Rural 2016;46:1824–9.
6. Gupta A, Manhas N, Raghubir R. Energy metabolism during cutaneous wound healing in immunocompromised and aged rats. Mol Cell Biochem 2004;259:9–14.
7. Moreno B, Bellido D, Sajoux I, Goday A, Saavedra D, Crujeiras AB, Casanueva FF. Comparison of a very low-calorie-ketogenic diet with a standard low-calorie diet in the treatment of obesity. Endocrine 2014;47:793–805.
8. Ruskin DN, Kawamura M, Masino SA. Reduced pain and inflammation in juvenile and adult rats fed a ketogenic diet. PLoS One 2009;4:e8349–e8349.
9. Masino SA, Geiger JD. Are purines mediators of the anticonvulsant/neuroprotective effects of ketogenic diets? Trends Neurosci 2008;31:273–8.

10. Moreno B, Crujeiras AB, Bellido D, Sajoux I, Casanueva FF. Obesity treatment by very low-calorie-ketogenic diet at two years: reduction in visceral fat and on the burden of disease. Endocrine 2016;54:681–90.

11. Masino SA, Kawamura M, Wasser CD, Pomeroy LT, Ruskin DN. Adenosine, ketogenic diet and epilepsy: the emerging therapeutic relationship between metabolism and brain activity. Curr Neuropharmacol 2009;7:257–68.

12. Shimazu T, Hirschey MD, Newman J, He W, Shirakawa K, Le Moan N, Grueter CA, Lim H, Saunders LR, Stevens RD, Newgard CB, Farese Jr R V, de Cabo R, Ulrich S, Akassoglou K, Verdin E. Suppression of oxidative stress by β-hydroxybutyrate, an endogenous histone deacetylase inhibitor. Science 2013;339:211–4.

13. Lu Y, Yang Y-Y, Zhou M-W, Liu N, Xing H-Y, Liu X-X, Li F. Ketogenic diet attenuates oxidative stress and inflammation after spinal cord injury by activating Nrf2 and suppressing the NF-κB signaling pathways. Neurosci Lett 2018;683:13–8.

14. Neal EG, Chaffe H, Schwartz RH, Lawson MS, Edwards N, Fitzsimmons G, Whitney A, Cross JH. The ketogenic diet for the treatment of childhood epilepsy: a randomised controlled trial. Lancet Neurol 2008;7:500–6.

15. Barañano KW, Hartman AL. The ketogenic diet: uses in epilepsy and other neurologic illnesses. Curr Treat Options Neurol 2008;10:410–9.

16. Storoni M, Plant GT. The Therapeutic Potential of the Ketogenic Diet in Treating Progressive Multiple Sclerosis. Mult Scler Int 2015;2015:681289.

17. Phinney SD. Ketogenic diets and physical performance. Nutr Metab (Lond) 2004;1:2.

18. Fomin DA, McDaniel B, Crane J. The promising potential role of ketones in inflammatory dermatologic disease: a new frontier in treatment research. J Dermatolog Treat 2017;28:484–7.

19. Fomin DA, Handfield K. The ketogenic diet and dermatology: a primer on current literature. Cutis 2020;105:40–3.

20. Gaertner DJ, Hallman TM, Hankenson FC, Batchelder MA. Anesthesia and analgesia for laboratory rodents. In: Fish, R.E., Danneman, P.J., Brown, M., Karas AZ, editor. Anesthesia and Analgesia in Laboratory Animals. 2nd ed. Elsevier Academic Press, London (UK); 2008:239–97.

21. Freeman JM, Kossoff EH, Hartman AL. The Ketogenic Diet: One Decade Later. Pediatrics 2007;119:535–43.

22. Kurokawa T, Itagaki S, Yamaji T, Nakata C, Noda T, Hirano T, Iseki K. Antioxidant Activity of a Novel Extract from Bamboo Grass (AHSS) against Ischemia-Reperfusion Injury in Rat Small Intestine. Biol Pharm Bull 2006;29:2301–3.

23. Guneli E, Cavdar Z, Islekel H, Sarioglu S, Erbayraktar S, Kiray M, Sokmen S, Yilmaz O, Gokmen N. Erythropoietin protects the intestine against ischemia/reperfusion injury in rats. Mol Med 2007;13:509–17.

24. Gamble M. The Hematoxylins and Eosin. In: Bancroft, JD and Gamble M, editor. Theory and Practice of Histological Techniques. 6th ed. Philadelphia: Churchill Livingstone Elsevier; 2008:121–34.

25. Jones ML, Bancroft JD, Gamble M. Connective Tissues and Stains. In: Bancroft, JD and Gamble M, editor. Theory and Practice of Histological Techniques. 6th ed. Philadelphia: Churchill Livingstone Elsevier; 2008:135–60.

26. Buchwalow IB, Böcker W. Working with Antibodies. In: Immunohistochemistry: Basics and Methods. Springer Berlin Heidelberg; 2010:31–9.

27. Masson-Meyers DS, Andrade TAM, Caetano GF, Guimaraes FR, Leite MN, Leite SN, Frade MAC. Experimental models and methods for cutaneous wound healing assessment. Int J Exp Pathol 2020;101:21–37.

28. Dawson B, Trapp RG. Basic & Clinical Biostatistics. In: Basic & Clinical Biostatistics. 4th ed. Lange Medical Books / McGraw-Hill Medical Publishing Division; 2004:162–89.

29. Kayode OT, Rotimi DE, Olaolu TD, Adeyemi OS. Ketogenic diet improves and restores redox status and biochemical indices in monosodium glutamate-induced rat testicular toxicity. Biomed Pharmacother 2020;127:110227.

30. Hamidi SA, Tabatabaei Naeini A, Oryan A, Tabandeh MR, Tanideh N, Nazifi S. Cutaneous Wound Healing after Topical Application of Pistacia atlantica Gel Formulation in Rats. Turkish J Pharm Sci 2017;14:65–74.

31. Li J, Liu Y, Liu H, Chen L, Li R. Ketogenic Diet Potentiates Electrical Stimulation–Induced Peripheral Nerve Regeneration after Sciatic Nerve Crush Injury in Rats. Mol Nutr Food Res 2020;64:1900535.

32. Park S, Zhang T, Wu X, Yi Qiu J. Ketone production by ketogenic diet and by intermittent fasting has different effects on the gut microbiota and disease progression in an Alzheimer's disease rat model. J Clin Biochem Nutr 2020;67:188–98.

33. Arnhold J. The Dual Role of Myeloperoxidase in Immune Response. Int J Mol Sci 2020;21:8057.

34. Hasmann A, Wehrschuetz-Sigl E, Marold A, Wiesbauer H, Schoeftner R, Gewessler U, Kandelbauer A, Schiffer D, Schneider KP, Binder B, Schintler M, Guebitz GM. Analysis of myeloperoxidase activity in wound fluids as a marker of infection. Ann Clin Biochem Int J Lab Med 2013;50:245–54.

35. Gabr SA, Alghadir AH. Evaluation of the Biological Effects of Lyophilized Hydrophilic Extract of Rhus coriaria on Myeloperoxidase (MPO) Activity, Wound Healing, and Microbial Infections of Skin Wound Tissues. Evid Based Complement Alternat Med 2019;2019:5861537.

36. Nguyen V-L, Truong C-T, Nguyen BCQ, Vo T-N Van, Dao T-T, Nguyen V-D, Trinh D-TT, Huynh HK, Bui C-B. Anti-inflammatory and wound healing activities of calophyllolide isolated from Calophyllum inophyllum Linn. PLoS One 2017;12:e0185674–e0185674.

37. Ebaid H, Ahmed OM, Mahmoud AM, Ahmed RR. Limiting prolonged inflammation during proliferation and remodeling phases of wound healing in streptozotocin-induced diabetic rats supplemented with camel undenatured whey protein. BMC Immunol 2013;14:31.

38. Poff AM, Ari C, Arnold P, Seyfried TN, D'Agostino DP. Ketone supplementation decreases tumor cell viability and prolongs survival of mice with metastatic cancer. Int J cancer 2014;135:1711–20.

39. Paoli A, Moro T, Bosco G, Bianco A, Grimaldi KA, Camporesi E, Mangar D. Effects of n-3 polyunsaturated fatty acids (ω-3) supplementation on some cardiovascular risk factors with a ketogenic Mediterranean diet. Mar Drugs 2015;13:996–1009.

40. Alshehabat M, Hananeh W, Ismail ZB, Rmilah SA, Abeeleh MA. Wound healing in immunocompromised dogs: A comparison between the healing effects of moist exposed burn ointment and honey. Vet world 2020;13:2793–7.

41. Wang AS, Armstrong EJ, Armstrong AW. Corticosteroids and wound healing: clinical considerations in the perioperative period. Am J Surg 2013;206:410–7.

42. Kesl S, Jung M, Prather J, Sherwood J, Gould L, D'Agostino D. Sustaining dietary ketosis to improve blood flow and wound healing in young and aged Fisher rats (734.7). FASEB J 2014;28.

43. Xue M, Jackson CJ. Extracellular Matrix Reorganization During Wound Healing and Its Impact on Abnormal Scarring. Adv wound care 2015;4:119–36.

44. Merjaneh M, Langlois A, Larochelle S, Cloutier CB, Ricard-Blum S, Moulin VJ. Pro-angiogenic capacities of microvesicles produced by skin wound myofibroblasts. Angiogenesis 2017;20:385–98.

45. Rani S, Ritter T. The Exosome - A Naturally Secreted Nanoparticle and its Application to Wound Healing. Adv Mater 2015;28:5542–52.

46. Shroff A, Mamalis A, Jagdeo J. Oxidative Stress and Skin Fibrosis. Curr Pathobiol Rep 2014;2:257–67.

47. Boison D. New insights into the mechanisms of the ketogenic diet. Curr Opin Neurol 2017;30:187–92.

48. Khodaeiani E, Fakhrjou A, Amirnia M, Babaei-Nezhad S, Taghvamanesh F, Razzagh-Karimi E, Alikhah H. Immunohistochemical evaluation of p53 and Ki67 expression in skin epithelial tumors. Indian J Dermatol 2013;58:181–7.

49. Mattern J, Büchler MW, Herr I. Cell Cycle Arrest by Glucocorticoids May Protect Normal Tissue and Solid Tumors from Cancer Therapy. Cancer Biol Ther 2007;6:1341–50.

50. de Pablo M. Determination of natural resistance of mice fed dietary lipids to experimental infection induced by Listeria monocytogenes. FEMS Immunol Med Microbiol 2000;27:127–33.

51. Chen L, Gajendrareddy PK, DiPietro LA. Differential expression of HIF-1α in skin and mucosal wounds. J Dent Res 2012;91:871–6.

52. Cury V, Moretti AIS, Assis L, Bossini P, Crusca J de S, Neto CB, Fangel R, de Souza HP, Hamblin MR, Parizotto NA. Low level laser therapy increases angiogenesis in a model of ischemic skin flap in rats mediated by VEGF, HIF-1α and MMP-2. J Photochem Photobiol B 2013;125:164–70.

53. Keshri GK, Gupta A, Yadav A, Sharma SK, Singh SB. Photobiomodulation with Pulsed and Continuous Wave Near-Infrared Laser (810 nm, Al-Ga-As) Augments Dermal Wound Healing in Immunosuppressed Rats. PLoS One 2016;11:e0166705–e0166705.

54. de Mayo T, Conget P, Becerra-Bayona S, Sossa CL, Galvis V, Arango-Rodríguez ML. The role of bone marrow mesenchymal stromal cell derivatives in skin wound healing in diabetic mice. PLoS One 2017;12:e0177533–e0177533.

55. Zhang Z, Zhao M, Wang J, Ding Y, Dai X, Li Y. Oral administration of skin gelatin isolated from Chum salmon (Oncorhynchus keta) enhances wound healing in diabetic rats. Mar Drugs 2011;9:696–711.

56. Puchowicz MA, Xu K, Sun X, Ivy A, Emancipator D, LaManna JC. Diet-induced ketosis increases capillary density without altered blood flow in rat brain. Am J Physiol Metab 2007;292:E1607–15.

الملخص العربى

النظام الغذائي الكيتوني يعزز التئام الجروح المتأخر في الجرذان التي تعاني من نقص المناعة: دراسة هستولوجية و هستوكيميائية مناعية

نهى رمضان محمد السويدى[١]، رشا عبد العزيز عبد اللطيف[٢]، مروة عوض عبد الحميد إبراهيم[١]

[١]قسم الهستولوجيا -[٢]قسم التشريح - كلية الطب - جامعة طنطا

مقدمة: التئام الجروح عملية معقدة يمكن أن تتأثر بعوامل مختلفة. تؤخر الستيرويدات القشرية عملية التئام الجروح بعدة آليات. يمكن أن يساعد النظام الغذائي الكيتوني في علاج العديد من الأمراض الجلدية خاصة تلك المرتبطة بالإجهاد التأكسدي.

الهدف من العمل: دراسة دور النظام الغذائي الكيتوني في تعزيز التئام الجروح المتأخر للجلد الرقيق في الفئران التي تعاني من نقص المناعة.

مواد و طرق البحث: تم توزيع أربع و عشرين من ذكور الجرذان البيضاء البالغة بالتساوي في أربع مجموعات: الضابطة ، الجرح الاستئصالي في الجرذان الطبيعية، الجرح الاستئصالي في الجرذان التي تعاني من نقص المناعة (٠,١ مجم / كجم / يوم من الديكساميثازون تحت الجلد لمدة ٣٠ يومًا) ، والجرح الاستئصالي في الجرذان التي تعاني من نقص المناعة مع النظام الغذائي الكيتوني (٧٥٪ دهون ، ٢٠٪ بروتين ، ٥٪ كربوهيدرات). تم الحصول على عينات الجرح في اليوم السابع أو الرابع عشر وتم معالجتها باستخدام تقنيات بيوكيميائية و هستولوجية و هستوكيميائية مناعية مختلفة.

النتائج: في كل من اليومين السابع والرابع عشر، أظهر جرح الجرذان التي تعاني من نقص المناعة زيادة ملحوظة في كل من المالونديالديهيد و الميلوبيروكسيديز النسيجي مقارنة بالفئران الطبيعية. كان متوسط مساحة الجرح أكبر بشكل ذي دلالة احصائية ، بينما انخفض متوسط معدل التئام الجروح وسماكة البشرة بشكل ذي دلالة احصائية مقارنة بالفئران الطبيعية. كان متوسط النسبة المئوية لمحتوى ألياف الكولاجين أعلى بشكل ذي دلالة احصائية مع انخفاض كبير في عدد خلايا Ki٦٧ الإيجابية و متوسط عدد الأوعية الدموية الموجبة للعامل VEGF.أظهر جرح الجرذان التي تعاني من نقص المناعة مع النظام الغذائي الكيتوني استعادة ذات دلالة احصائية لمعظم العوامل المدروسة خاصة في اليوم الرابع عشر.

الاستنتاجات: عزز النظام الغذائي الكيتوني التئام الجروح المتأخر عن طريق قمع الإجهاد التأكسدي، وتعديل الالتهاب وترسب الكولاجين، وتعزيز النكاثر، وتعزيز الأوعية الدموية خاصة في اليوم الرابع عشر.